

Mass Spectrometric Identification of Au₆₈(SR)₃₄ Molecular Gold Nanoclusters with 34-Electron Shell Closing

Amala Dass*

Department of Chemistry and Biochemistry, University of Mississippi, University, Mississippi 38677

Received June 9, 2009; E-mail: amal@olemiss.edu

Molecular gold nanoclusters (<2 nm, <200 atoms) contain a distinct number of core gold atoms and surface thiolate ligands. This is in contrast to the polydisperse, broad size distribution portrayed by transmission electron microscopy (TEM) images of larger Au nanocrystals (5–100 nm). Whetten's seminal work¹—weighing the nanocluster in a mass spectrometer—and more recent high resolution studies^{2–6} facilitated the identification of molecular nanoclusters such as Au₂₅(SR)₁₈, Au₃₈(SR)₂₄, and Au₁₄₄(SR)₅₉. These ubiquitous size-selected molecules display extraordinary stability^{4,7} and have been explained by electron shell closures.⁸ Other adjacent core sizes such as Au₂₄, Au₂₆, etc. are not readily synthesized experimentally and hence deemed unstable. X-ray crystallography has revealed the identity of Au₁₀₂(SR)₄₄⁹ and Au₂₅(SR)₁₈.^{10,11} These molecular nanoclusters display size-dependent optical^{12,13} and electrochemical^{14,15} properties and have been studied by theoretical calculations.^{16–19} Here the molecular formula Au₆₈(SR)₃₄ of the nanocluster commonly referred to as the 14 kDa species is identified using matrix assisted laser desorption/ionization time-of-flight (MALDI-TOF) mass spectrometry, and its stability is attributed to the 34-electron count shell closure.

Mass spectrometry revealed the presence of several size-selected clusters such as 5, 8, 14, 22, and 28 kDa Au cores.^{13,20,21} Facile syntheses and developments in mass spectrometry led to the assignments of 5, 8, and 28 kDa cores to Au₂₅,^{22–25} Au₃₈,^{4,26,27} and Au₁₄₄,²⁸ respectively. However, the identification of the molecular formula of nanoclusters of other sizes such as the 14 kDa species has been impeded by two factors: (a) difficulty in obtaining a sufficient amount of the nanocluster during synthesis; (b) lack of suitable analytical tools for characterization at high mass range. In this work, the 14 kDa species was successfully assigned with the molecular formula Au₆₈(SR)₃₄. Specifically Au₆₈ enriched samples were synthesized, when the rate of growth is “effectively halted, at certain levels of aggregation,”²⁹ i.e., 3 h of reaction time. Employing threshold laser fluence and use of DCTB (*trans*-2-[3-(4-*tert*-butylphenyl)-2-methyl-2-propenylidene]malononitrile) as a MALDI matrix enabled the ion formation and detection of the Au₆₈(SR)₃₄ molecular ions.

Briefly, based on a previous report,²⁵ 0.517 g (1.3 mmol) of HAuCl₄ was dissolved in 50 mL of THF and cooled in an ice bath for 30 min. 6.53 mmol (0.88 mL) of phenylethane thiol were added and stirred overnight. 10 mL of aq. NaBH₄ (0.57 g, 15 mmol) were added to the reaction instantaneously, and the reaction was continued for 3 h. The reaction mixture was concentrated, and the products were precipitated by the addition of water. The as-prepared nanoclusters are found to be enriched in Au₆₈. Isolation of pure nanocluster proved to be difficult and is being pursued in a separate study. In this work, the identity of the Au₆₈(SCH₂CH₂Ph)₃₄ nanocluster is reported using mass spectrometry.

Figure 1 shows the intact molecular ion of the Au₆₈(SCH₂CH₂Ph)₃₄ nanocluster obtained in a positive linear mode of MALDI-TOF mass spectrometer. The other lower mass peaks

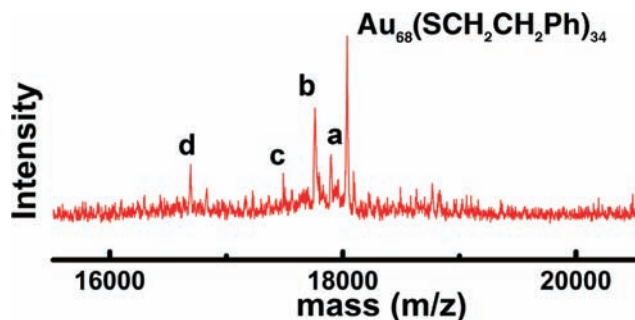


Figure 1. Positive linear mode MALDI-TOF mass spectrum of the as-prepared nanoclusters using DCTB (*trans*-2-[3-(4-*tert*-butylphenyl)-2-methyl-2-propenylidene]malononitrile) matrix and operating at threshold laser fluence. The molecular ion of the Au₆₈(SR)₃₄ nanocluster is the most intense peak. Peaks a, b, c, and d represent Au₆₈(SR)₃₃, Au₆₈(SR)₃₂, Au₆₈(SR)₃₀, and Au₆₄(SR)₃₀ fragments, respectively.

were assigned to Au₆₈(SR)₃₃, Au₆₈(SR)₃₂, Au₆₈(SR)₃₀, and Au₆₄(SR)₃₀ fragments. Cocrystallizing the nanocluster analyte with the DCTB matrix and ionization at threshold laser fluence was necessary to obtain the molecular peaks.

The stability of molecular nanoclusters has been intriguing. Recent work⁸ has provided a convincing, unified view of the molecular nanoclusters as superatom complexes invoking electron shell closure principles. Dips in experimental electron affinity values are found for 8, 14, 20, 34, and 58 electrons and are thought to lead to the closing of shells or subshells in gold clusters.³⁰ The shell-closing electron count (n^*) for molecular nanoclusters is calculated from the equation⁸

$$n^* = N\nu_A - M - z$$

where n^* is the shell-closing electron count, z is the charge state of the nanocluster, N is the number of core gold atoms, ν_A is the atomic valence, and M is the number of electron localizing ligands. The charge neutral Au₆₈(SR)₃₄ nanocluster would satisfy a 34-electron shell closure known for its exceptional stability. Other electron shell closures such as 8 and 58 have explained the stability of Au₂₅(SR)₁₈[−] and Au₁₀₂(SR)₄₄ species. A 14-electron count of a neutral Au₃₈(SR)₂₄ species matches the dip found at the 14 atom count for electron affinity.³⁰

The 14 kDa nanoclusters were predicted to have ~75 core atoms based on atomistic modeling of energy and structures in combination with experimental powder X-ray diffraction (XRD) data.³¹ Laser desorption mass spectra show a broad peak at 14 kDa which was approximated to ~75 core atom species.^{13,32,33} Based on broad LDI peaks with an fwhm of 3000 Da, it is difficult to exactly identify the number of core atoms or distinguish between 75 core atoms versus the Au₆₈ nanocluster. Since detailed mass spectrometric and XRD measurements have enabled the assignments for

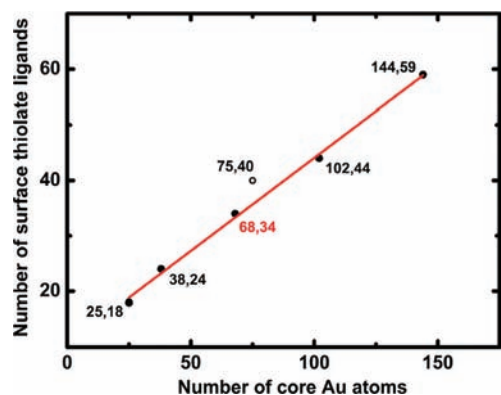


Figure 2. A plot of the number of surface thiolate ligands versus the number of core gold atoms for $\text{Au}_{25}(\text{SR})_{18}$, $\text{Au}_{38}(\text{SR})_{24}$, $\text{Au}_{68}(\text{SR})_{34}$, $\text{Au}_{102}(\text{SR})_{44}$, $\text{Au}_{144}(\text{SR})_{59}$ shown as filled circles (slope = 0.33; intercept = 10.46, $r^2 = 0.997$). $\text{Au}_{75}(\text{SR})_{40}$ (open circle; not used in the fit) does not fall on the straight line. Including the (75,40) data point in the correlation reduces the r^2 value to 0.977.

25, 38, 102, and 144 nanoclusters, it is possible to (a) check whether a correlation exists between the number of Au core atoms and surface thiolate ligands and (b) verify whether Au_{68} nanoclusters fall on the curve fit.

Figure 2 shows a linear correlation between the number of core Au atoms and surface thiolate ligands for 25, 38, 68, 102, and 144 nanoclusters. While removing $\text{Au}_{68}(\text{SR})_{34}$ from the data set retains the r^2 value at 0.997, inclusion of the (75,40) data point brings the correlation down to 0.977 (Figure S6). This shows that $\text{Au}_{68}(\text{SR})_{34}$ is a better fit with the rest of the known core sizes. Previously reported crystal structures^{9–11,34} of Au_{102} and Au_{25} show that the central Au core is protected by single [-SR-Au-SR-] and double [-SR-Au-SR-Au-SR-] staple motifs. The 102 and 25 clusters have 2 and 6 double staple motifs, respectively. $\text{Au}_{68}(\text{SR})_{34}$ being in the intermediate region is estimated to have 11 single and 4 double staple motifs which leaves a 49 atom Marks Decahedral core (Table S1).

It is not trivial to assign peaks at high mass range such as ~18 kDa. LDI-MS analysis¹ of gold nanoclusters lead to extensive fragmentation and is not suitable for assignment of nanoclusters. Murray and co-workers⁵ have shown that *matrix assisted* LDI-MS can be used to ionize and detect intact molecular ion peaks at ~7 kDa. Can MALDI-MS be useful in a higher mass region? First, the Au_{68} molecular peak shows a good fit between the experimental and calculated peaks (Figure S4). Second, a general trend of Au_4L_4 loss is observed in Au_{25} , Au_{38} , and Au_{68} nanoclusters consistent with earlier results. Third, successful assignments of four other closely related fragments peaks such as $\text{Au}_{68}(\text{SR})_{33}$, $\text{Au}_{68}(\text{SR})_{32}$, $\text{Au}_{68}(\text{SR})_{30}$, and $\text{Au}_{64}(\text{SR})_{30}$ have been made (Figure S1 inset). Fourth, negative mode spectra gave similar results eliminating any contributions from counterions. These results show that MALDI-MS is indeed reliable at a higher mass range and attest to the unambiguous nature of the $\text{Au}_{68}(\text{SR})_{34}$ assignment. Additional supportive evidence is provided by UV-vis data (Figure S5) of the Au_{68} enriched sample which shows an exponential decay curve with some step-like features in agreement with previous literature.¹³

In conclusion, the molecular formula $\text{Au}_{68}(\text{SCH}_2\text{CH}_2\text{Ph})_{34}$ has been assigned to the 14 kDa nanocluster using MALDI-TOF mass spectrometry. The 34-electron shell closing in a macroscopically obtained thiolated gold nanocluster is demonstrated. The Au_{68} nanocluster is predicted to have a 49 atom Marks decahedral core

with 19 inner core atoms and 30 outer atoms chelating with the staple motifs. The nanoclusters' predicted³⁵ formulation is $[\text{Au}]_{19+30} [\text{Au}(\text{SR})_2]_{11} [\text{Au}_2(\text{SR})_3]_4$.

Acknowledgment. This research was supported by University of Mississippi, Department of Chemistry and Biochemistry and the office of sponsored research. I thank Thomas Krick for his assistance with MALDI-TOF measurements as well as Keith Hollis and Gregory Tschumper for helpful discussions.

Supporting Information Available: Detailed expanded mass spectra. This material is available free of charge via the Internet at <http://pubs.acs.org>.

References

- Whetten, R. L.; Khoury, J. T.; Alvarez, M. M.; Murthy, S.; Vezmar, I.; Wang, Z. L.; Stephens, P. W.; Cleveland, C. L.; Luedtke, W. D.; Landman, U. *Adv. Mater.* **1996**, *8*, 428–433.
- Negishi, Y.; Nobusada, K.; Tsukuda, T. *J. Am. Chem. Soc.* **2005**, *127*, 5261–5270.
- Tracy, J. B.; Kalyuzhny, G.; Crowe, M. C.; Balasubramanian, R.; Choi, J. P.; Murray, R. W. *J. Am. Chem. Soc.* **2007**, *129*, 6706–6707.
- Chaki, N. K.; Negishi, Y.; Tsunoyama, H.; Shichibu, Y.; Tsukuda, T. *J. Am. Chem. Soc.* **2008**, *130*, 8608–8610.
- Dass, A.; Stevenson, A.; Dubay, G. R.; Tracy, J. B.; Murray, R. W. *J. Am. Chem. Soc.* **2008**, *130*, 5940–5946.
- Dass, A.; Dubay, G. R.; Fields-Zinna, C. A.; Murray, R. W. *Anal. Chem.* **2008**, *80*, 6845–6849.
- Shichibu, Y.; Negishi, Y.; Tsunoyama, H.; Kanehara, M.; Teranishi, T.; Tsukuda, T. *Small* **2007**, *3*, 835–839.
- Walter, M.; Akola, J.; Lopez-Acevedo, O.; Jadzinsky, P. D.; Calero, G.; Ackerson, C. J.; Whetten, R. L.; Gronbeck, H.; Hakkinen, H. *Proc. Natl. Acad. Sci. U.S.A.* **2008**, *105*, 9157–9162.
- Jadzinsky, P. D.; Calero, G.; Ackerson, C. J.; Bushnell, D. A.; Kornberg, R. D. *Science* **2007**, *318*, 430–433.
- Heaven, M. W.; Dass, A.; White, P. S.; Holt, K. M.; Murray, R. W. *J. Am. Chem. Soc.* **2008**, *130*, 3754–3755.
- Zhu, M.; Aikens, C. M.; Hollander, F. J.; Schatz, G. C.; Jin, R. *J. Am. Chem. Soc.* **2008**, *130*, 5883–5885.
- Alvarez, M. M.; Khoury, J. T.; Schaaff, T. G.; Shafiqullin, M. N.; Vezmar, I.; Whetten, R. L. *J. Phys. Chem. B* **1997**, *101*, 3706–3712.
- Schaaff, T. G.; Shafiqullin, M. N.; Khoury, J. T.; Vezmar, I.; Whetten, R. L.; Cullen, W. G.; First, P. N.; Gutierrez-Wing, C.; Ascencio, J.; JoseYacamán, M. J. *J. Phys. Chem. B* **1997**, *101*, 7885–7891.
- Quinn, B. M.; Liljeroth, P.; Ruiz, V.; Laaksonen, T.; Kontturi, K. *J. Am. Chem. Soc.* **2003**, *125*, 6644–6645.
- Murray, R. W. *Chem. Rev.* **2008**, *108*, 2688–2720.
- Akola, J.; Walter, M.; Whetten, R. L.; Hakkinen, H.; Gronbeck, H. *J. Am. Chem. Soc.* **2008**, *130*, 3756–3757.
- Jiang, D. E.; Tiago, M. L.; Luo, W. D.; Dai, S. *J. Am. Chem. Soc.* **2008**, *130*, 2777–2779.
- Aikens, C. M. *J. Phys. Chem. C* **2008**, *112*, 19797–19800.
- Mednikov, E. G.; Dahl, L. E. *Small* **2008**, *4*, 534–537.
- Schaaff, T. G.; Knight, G.; Shafiqullin, M. N.; Borkman, R. F.; Whetten, R. L. *J. Phys. Chem. B* **1998**, *102*, 10643–10646.
- Schaaff, T. G.; Shafiqullin, M. N.; Khoury, J. T.; Vezmar, I.; Whetten, R. L. *J. Phys. Chem. B* **2001**, *105*, 8785–8796.
- Donkers, R. L.; Lee, D.; Murray, R. W. *Langmuir* **2004**, *20*, 1945–1952.
- Donkers, R. L.; Lee, D.; Murray, R. W. *Langmuir* **2008**, *24*, 5976–5976.
- Zhu, M.; Lanni, E.; Garg, N.; Bier, M. E.; Jin, R. *J. Am. Chem. Soc.* **2008**, *130*, 1138–1139.
- Wu, Z.; Suhan, J.; Jin, R. *J. Mater. Chem.* **2009**, *19*, 622–626.
- Toikkanen, O.; Ruiz, V.; Ronholm, G.; Kalkkinen, N.; Liljeroth, P.; Quinn, B. M. *J. Am. Chem. Soc.* **2008**, *130*, 11049–11055.
- Qian, H.; Zhu, M.; Andersen, U. N.; Jin, R. *J. Phys. Chem. A* **2009**, *113*, 4281–4284.
- Hicks, J. F.; Miles, D. T.; Murray, R. W. *J. Am. Chem. Soc.* **2002**, *124*, 13322–13328.
- Alvarez, M. M.; Khoury, J. T.; Schaaff, T. G.; Shafiqullin, M.; Vezmar, I.; Whetten, R. L. *Chem. Phys. Lett.* **1997**, *266*, 91–98.
- Taylor, K. J.; Pettiettehall, C. L.; Cheshnovsky, O.; Smalley, R. E. *J. Chem. Phys.* **1992**, *96*, 3319–3329.
- Cleveland, C. L.; Landman, U.; Schaaff, T. G.; Shafiqullin, M. N.; Stephens, P. W.; Whetten, R. L. *Phys. Rev. Lett.* **1997**, *79*, 1873–1876.
- Schaaff, T. G.; Whetten, R. L. *J. Phys. Chem. B* **1999**, *103*, 9394–9396.
- Balasubramanian, R.; Guo, R.; Mills, A. J.; Murray, R. W. *J. Am. Chem. Soc.* **2005**, *127*, 8126–8132.
- Zhu, M.; Eckenhoff, W. T.; Pintauer, T.; Jin, R. *J. Phys. Chem. C* **2008**, *112*, 14221–14224.
- Pei, Y.; Gao, Y.; Zeng, X. C. *J. Am. Chem. Soc.* **2008**, *130*, 7830–7832.

JA904713F